

An empirical model for landslide travel distance prediction in Wenchuan earthquake area

Abstract Sliding mass of landslides highly endangered the area along travel path, especially landslides with long travel distance. It is necessary to develop an effective prediction model for preliminarily evaluating landslide travel distance so as to improve disaster prevention and relocation. This paper collected 54 landslides with 347–4,170 m travel distance triggered by the 2008 Wenchuan earthquake to discuss the effectiveness of various influential factors on landslide travel distance and obtained an empirical model for its prediction. The results revealed that rock type, sliding source volume, and slope transition angle were the predominant factors on landslide travel distance. The validity of proposed model was verified by the satisfactory agreement between observations and predictions. Therefore, this model might be practically applicable in Wenchuan earthquake area and other similar geomorphological and geological regions.

Keywords Landslide · Travel distance prediction · Statistical analysis · Influential factors · Wenchuan earthquake

Introduction

Landslide is a major geomorphological process affecting landscape evolution in mountainous area (Roering et al. 2005); it may be triggered by rainfall or earthquake. During the 2008 Wenchuan earthquake, 197,481 slope failures were triggered in about 110,000 km² (Xu et al. 2013), about 20,000 deaths were attributed to landslides (Huang and Li, 2008, 2009a). Numerous authors have analyzed the relations between landslide spatial distribution and influential factors so as to serve landslide hazard map (Huang and Li 2009a, b; Xu et al. 2009b, 2010; Chigira et al. 2010; Qi et al. 2010; Dai et al. 2011; Gorum et al. 2011; Guo and Hamada 2013). However, there are few studies having explored the effectiveness of various factors on landslide travel distance and its prediction in Wenchuan earthquake area, except that Qi et al. (2011) delineated six typical destructive long travel landslides and listed 66 valuable cases, but this research was limited to analyze the relationship between elevation loss and sliding area and travel distance. Yin et al. (2009) pointed out that at least 4,970 sites were highly potential to develop into geo-hazards. Therefore, if it was possible to preliminarily estimate landslide travel distance and endangered area, besides landslide spatial distribution, the quality of landslide hazard map would be highly improved and more applicable to disaster mitigation and relocation.

However, landslide travel distance prediction is a complicated issue because it was governed by the properties of materials (i.e., grain size distribution and water content), topographical factors, mobile mechanics of failed mass, the confinement attribute of travel path, and so on. In order to research this topic to mitigate geo-hazard caused by landslide, there are three techniques to evaluate landslide travel distance: empirical model (for example, Rickenmann 1999, 2005; Legros 2002), theoretical model (for example, Takahashi 1981, 1991), and numerical simulation model (for example, McDougall and Hungr 2003). Theoretical model

requires two parameters which are difficult to be accurately estimated, that is, velocity of sliding mass and frictional parameter, whereas the predictive result of numerical simulation model highly depends on input data, which would be variable during sliding process. Simplifying assumptions are often made for theoretical model and numerical simulation model, especially where input parameters cannot be measured easily.

Since the parameters of a landslide may change during movement to avoid the usage of uncertainly and highly variable parameters to predict landslide travel distance, empirical model was widely applied to preliminary assessment of landslide travel distance, as a result of no requirement of the parameters of rheology or detail mechanics of movement, besides, it is a relatively simple tool to offer a practical means of prediction. Hence, there are lots of previous researches to use this approach, such as Scheidegger 1973; Corominas 1996; Fannin and Wise 2001; Hunter and Fell 2003; Okura et al. 2003; Berti and Simoni 2007; Prochaska et al. 2008; Hattanji and Moriwaki 2009, 2011. Among these studies, a common index for expressing landslide mobility was widely used and firstly designated by Heim (1932) as *fahrböschung*, which is the angle of the line connecting the head of sliding source and the toe of the deposited mass. Shreve (1968) and Scheidegger (1973) later called the tangent of this angle as equivalent coefficient of friction. More recently, some authors named this angle as angle of reach (Corominas 1996) or travel distance angle (Hunter and Fell 2003). Further, equivalent coefficient of friction has a significant correlation with landslide volume, as demonstrated by Scheidegger (1973), Corominas (1996), Fannin and Wise (2001), Rickenmann (1999, 2005) and also has a significant correlation with slope angle (Hunter and Fell 2003; Hattanji and Moriwaki 2009, 2011). However, these previous studies neither have revealed the comprehensive relationship between landslide travel distance and various influential factors nor have discussed the effectiveness of each influential factor on travel distance. Hence, a new model is needed to consider more influential factors on landslide travel distance simultaneously. Finlay et al. (1999) made use of multiple regression model to study over 1,100 man-modified slopes in Hong Kong; however, most of these landslide scales and travel distances are much smaller than those landslides from natural slopes. Meanwhile, most of previous researches were about non-seismically induced landslides; therefore, it is meaningful to explore the prediction of earthquake-induced landslide travel distance by simultaneously taking numerous influential factors into consideration.

This paper collected 54 well-documented landslides triggered by the 2008 Wenchuan earthquake to study the relations between landslide travel distance and six influential factors. It was divided into six sections and proceeded as follows: section 2 introduced the data source, section 3 reported the relations between landslide travel distance and landslide characteristic parameters, section 4 analyzed the effectiveness of influential factors on landslide travel distance and developed a new model to its prediction, and section

5 and section 6 presented the discussions and conclusions, respectively.

Data selection of landslide and its parameters

In this paper, the collected data excluded not only landslides obstructed by relatively large river, valley, and infrastructures but also travel path sharply confined by steep lateral slope and landslides with big deflection travel path, as a result of that, the attributes of travel path had significant effect on the mobilization of failed mass (Shaller 1991; Corominas, 1996). However, the characteristics of confinement are difficult to be quantitatively expressed. Hence, the travel path of selected landslides was relatively open or confined by gentle lateral slope and the travel path with relatively small deflection. Totally, 54 landslides were collected based on remote sensing interpretation, field investigation, and descriptions of published papers and books. The source volume range of these landslides is 4.5×10^4 – 2.75×10^7 m³; horizontal travel distance is within 347–4,170 m.

Figure 1 illustrates the basic terminologies and notations. The longitudinal profile of a slope was obtained by using topographic map. Based on the density of contour lines, slope was divided into several segments. Contour lines appear relatively sparser; the inclination of corresponding segment will be smaller and the contour lines become much denser; the corresponding segment has relatively larger slope angle. The interval changing segments of contour lines (marked by ellipse in Fig. 1) along longitudinal section correspond with the inclination changing segments along a slope. The boundary of contour line interval apparent changing

in the topographic map along slope longitudinal section was regarded as the turning point of different segments of a slope; hence, a slope will be divided into several segments, and the average inclination and slope height of each segment will be obtained. Slope angle, θ , is the average inclination of the sectional slope with failed part. Slope height, h , is the elevation difference of the sectional slope with failed part. Travel distance, L_{\max} , is the horizontal distance between the crest of the sliding source and the distal of debris. Landslide height, H_{\max} , is the maximum elevation loss between sliding source and debris. α represents fahrböschung (Heim 1932) or travel distance angle (Hunter and Fell 2003). Slope transition angle, β , is the angle between the upper slope (failed section) and lower slope, indicating the change degree of slope inclination. During investigation, the area of sliding source, in situ outlined on the map, was calculated by ArcGIS software, and the volume of sliding source was obtained from multiplying the area of sliding source by average collapse depth. The average collapse depth was estimated from typical longitudinal profile of slope, as shown in Fig. 2. According to the rock strength and weathered degree, rock materials were assorted into two types, such as hard rock and soft rock, further divided into two subclasses, respectively, as listed in Table 1.

Topographical factors play an important role in the mobilization of landslide (Okura et al. 2003). The topography of a slope can be described by slope angle (θ), slope transition angle (β), and slope height (h). Slope angle has positive correlation between internal friction coefficient (Okura et al. 2003), which decides the energy consumption by internal friction; meanwhile,

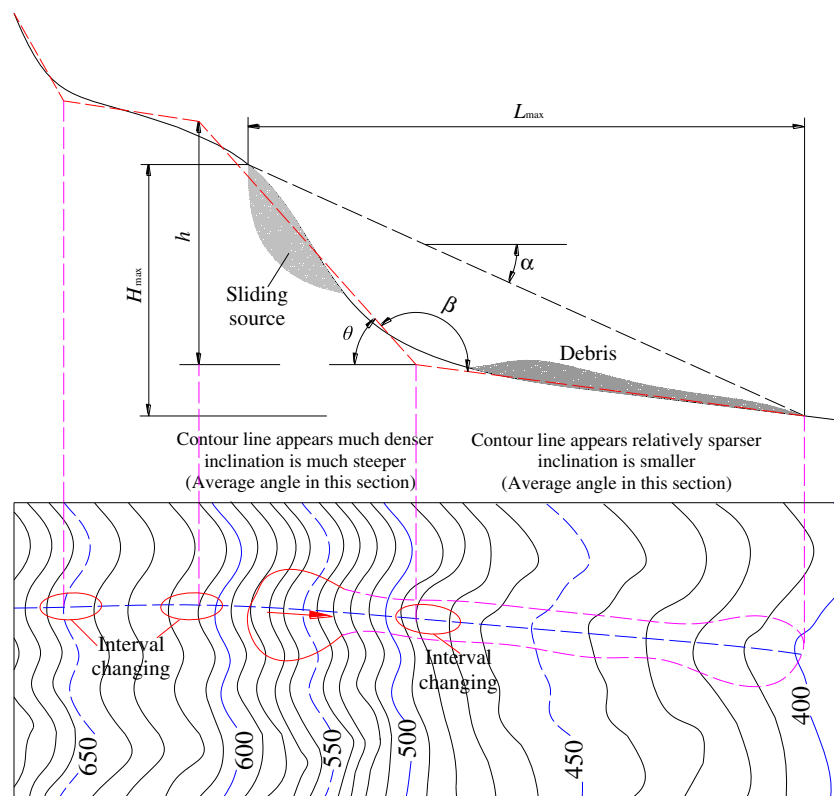


Fig. 1 The sketch of landslide for the definitions of geometric parameters

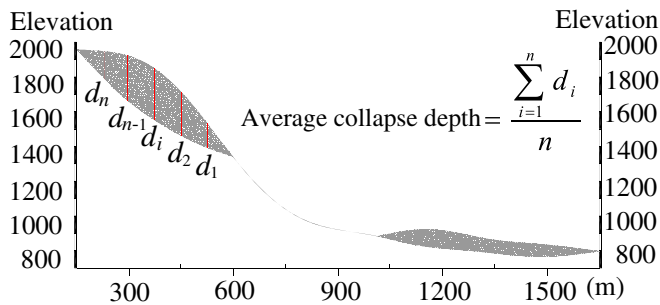


Fig. 2 Typical longitudinal profile of landslide

the steeper the slope is, the bigger the component of gravity to accelerate the sliding mass is and higher consumption of kinetic energy due to the impact at the foot of upper slope. The changing degree of slope inclination between upper slope and lower slope can be expressed by slope transition angle (β), which has a strong effect on the impact of sliding mass; it will affect the postimpact mobile motion of sliding mass. For slope height (h), it implies the preimpact potential energy of sliding mass and governs the available space to accelerate the failed mass; the bigger slope height, the faster sliding velocity; the larger kinetic energy was consumed during impact at the slope transition section.

The influence of seismic wave on landslide travel distance was explored in terms of energy by Kokusho et al. (2007, 2009). Furthermore, Wang and Lin (2011) researched seismic effect on landslide initiation and displacement by shaking model test and proposed that “the final runout displacement is not proportional with the relationship of law of similitude but can be obtained from a normalized displacement relationship with maximum loading amplitude.” Since peak ground acceleration is one of the most important parameters to represent seismic energy, and horizontal peak ground acceleration was widely used to evaluate slope stability; hence, horizontal peak ground acceleration (PHA) was applied during the following study about influential factors on landslide travel distance, but it is impossible to install monitoring equipment at each investigated landslide before Wenchuan earthquake, so PHAs of landslides were estimated by Eq. (1), which

was derived from 183 seismic stations and considered hanging-foot wall effect (Guo and Hamada 2013).

$$\ln \text{PHA} = a_1 \ln(D_{\text{rup}} + a_2) + a_3 D_{\text{rup}} + a_4 \quad (1)$$

Where PHA is the horizontal peak ground acceleration (centimeters per square second); D_{rup} represents nearest distance from site to Yingxiu-Beichuan surface fault rupture (kilometer) located by using USGS result (Ji and Hayes, 2008); and a_1 , a_2 , a_3 , and a_4 are the regression coefficients, listed in Table 2, in which R^2 stands for coefficient of determination.

The distribution of 46 landslides was illustrated in Fig. 3, and their parameters were listed in Table 3, which were used to obtain statistical model for landslide travel distance. Other eight landslides were applied to verify the validity of proposed statistical model in following section 4.

Relationships between landslide travel distance and landslide parameters

Figures 4 and 5 illustrate the relations between landslide travel distance and sliding source volume and area, respectively; nevertheless, the statistical significance levels are relatively weak; these two results both suggest that landslide travel distance had exponential correlation with landslide scale (sliding source volume and area); it means landslide travel distance would generally and rapidly increase with landslide scale. Figure 6 illustrates that horizontal travel distance (L_{max}) had a relatively strong linear correlation with landslide height (H_{max} , total elevation loss). The relation between landslide horizontal travel distance and landslide height were further explored based on nonvolcanic and volcanic landslides (Hayashi and Self 1992; Legros 2002), as shown in Fig. 7, which also suggests that landslide travel distance increased with the elevation loss of failed mass. The reason was attributed to that failed mass was forced to travel down by gravity, and the potential energy was transformed to kinetic energy.

Statistical model of landslide travel distance

Although landslide travel distance (L_{max}) had a relatively significant correlation with landslide height (H_{max}) in Fig. 6, it

Table 1 Classification standard of rock type (Chang et al. 2006)

Rock type	Weathered degree and typical rock		Uniaxial compression strength (σ , MPa)
Hard rock	RT1	Non-weathered ~ slightly weathered magmatic rock, diorite, basalt, andesite, gneiss, and quartzite, etc.	$\sigma > 60$
	RT2	Non-weathered ~ slightly weathered marble, slate, limestone, dolomite, metamorphic quartz rock, etc. Moderately weathered magmatic rock, diorite, basalt, andesite, gneiss, and quartzite, etc.	$30 < \sigma \leq 60$
Soft rock	RT3	Non-weathered or slightly weathered tuff, phyllite, marl, sandy mudstone, etc. Moderately ~ strongly weathered hard rock	$15 < \sigma \leq 30$
	RT4	Non-weathered ~ slightly weathered shale, mudstone, shaly sand, etc. Strongly weathered hard rock Moderately ~ strongly weathered tuff, phyllite, marl, sandy mudstone, etc.	$\sigma \leq 15$

Table 2 Regression parameters of seismic acceleration attenuation (Guo and Hamada 2013)

Hanging wall or footwall	a_1	a_2	a_3	a_4	R^2
Hanging wall	-0.8203	13.767	-0.0042	9.169	0.64
Footwall	-0.6907	5.618	-0.0072	7.939	0.55

cannot be used to predict landslide travel distance because the stop place of failed mass and the top of sliding source were both unaware before landslide occurrence. Since landslide movement was affected by numerous factors, hence, the predictive model of landslide travel distance had better consider as many influential factors as possible simultaneously. Under the linear assumption, multiple linear regression and backward elimination approach were applied to obtain optimization model of landslide travel distance in the aid of F test and t test. The regression procedures and results were listed in Table 4.

In Table 4, L_{max} refers to landslide horizontal travel distance (meters); RT refers to rock type, it was qualitatively considered and 4, 3, 2, and 1 were, respectively, assigned to RT1, RT2, RT3, and RT4; V represents the volume of sliding source (cubic meter); β represents slope transition angle ($^\circ$); h represents slope height of the sectional slope with failed part (meters); PHA refers to horizontal peak ground acceleration (meters per square second) estimated from Eq. (1); and θ denotes slope angle of the sectional slope with failed part ($^\circ$). The basis of logarithm is 10. Multiple R means multiple correlation coefficient, which represents the correlated level between dependent variable and independent variables. F -stat denotes regressive F value, $F_{0.05}$ denotes F test threshold value with 95 % significance level. If F -stat is bigger than $F_{0.05}$, it suggests overall regression of the model satisfies statistical significance level. t -stat denotes regressive t value of each regression coefficient, $t_{0.05}$ denotes t test threshold value with 95 % significance level; if t -stat is larger than $t_{0.05}$, it suggests

corresponding regression coefficient, n_i , which satisfies significance level of regression. However, not all regression coefficients have statistical significance during regression procedures; therefore, the variable with smallest absolute t -stat value (bold digit in Table 4) was eliminated and then re-regressed step by step until overall regression of the model and all regressive coefficients both satisfy statistical significance level. These procedures are named as backward elimination regression. Because the units of independent variables affect regression coefficient, n_i , therefore, standardized regression coefficient, n'_i , was applied to exclude the effect of unit dimension, so as to have insight into the effectiveness of each independent variable (influential factors) on dependent variable (landslide travel distance).

Compared to four models in Table 4, F tests suggest that all of these hypothetical models have statistical significance and satisfy linear assumption. Based on backward elimination procedures and those absolute values of each standardized regression coefficient in six variables model, they both suggest that rock type, sliding source volume, and slope transition angle were more influential than slope height, seismic acceleration, and slope angle on landslide travel distance. Furthermore, the optimization model with three variables satisfies not only overall statistical significance (F -test) but also the significance of each regression coefficient (t test), listed in Table 4, the empirical model for predicting landslide travel distance based on presented dataset in Wenchuan earthquake area was shown as Eq. (2):

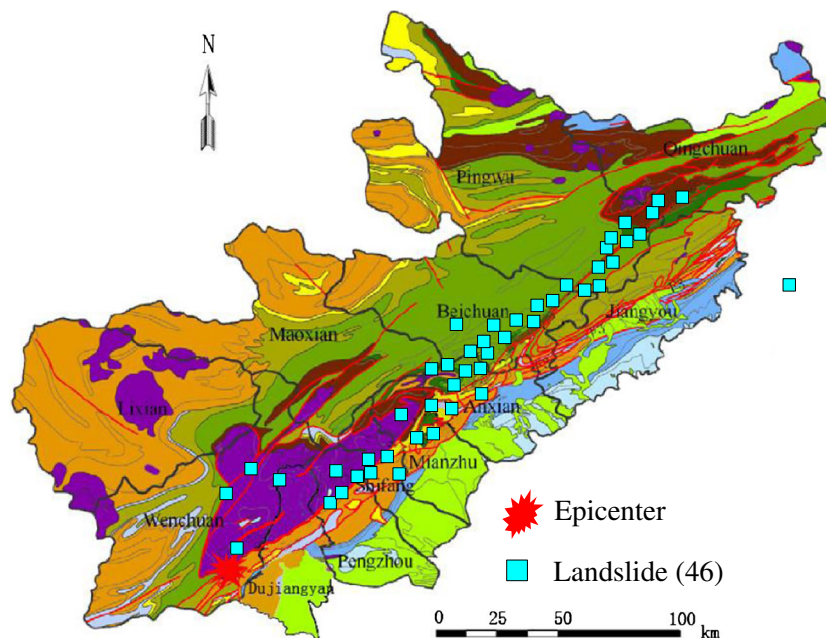
**Fig. 3** The distribution of 46 landslides (based on Qi, et al. 2011)

Table 3 The parameters of 46 landslides induced by the 2008 Wenchuan earthquake

No.	Latitude, longitude	Slope angle, θ ($^{\circ}$)	Slope transition angle, β ($^{\circ}$)	Slope height, h (m)	The volume of sliding source, V (m^3)	The area of sliding source, A (m^2)	Travel distance, L_{max} (m)	Landslide height, H_{max} (m)	PHA (m/s^2)	Rock type, RT	Predicted L_{rmax} (m)	Error (%)	Landslide type	Reference
1	N31.563, E103.703	25	173	481	1.200E+07	2.857E+06	725	338	4.082	RT3	911.09	25.67 %	Soil slide	Li et al. 2010; Li and Kong 2010
2	N31.293, E103.848	40	170	361	2.430E+06	1.620E+05	710	386	5.373	RT2	1029.44	44.99 %	Rock slide	Li et al. 2009, 2010; Li and Kong 2010
3	N32.055, E104.678	31	165	260	1.954E+06	1.149E+05	547	222	7.556	RT3	806.59	47.46 %	Rock slide	Li et al. 2009, 2010; Li and Kong 2010
4	N32.227, E104.865	30	162	481	1.920E+07	4.800E+05	843	400	6.754	RT3	1233.25	46.29 %	Rock slide	Li et al. 2009, 2010; Li and Kong 2010
5	N32.181, E104.814	42	167	301	8.775E+05	2.925E+05	378	335	6.935	RT4	498.33	31.83 %	Soil slide	
6	N32.086, E104.658	35	166	254	2.022E+06	2.528E+05	347	243	6.503	RT4	580.96	67.42 %	Soil slide	Li et al. 2010; Li and Kong 2010
7	N32.412, E105.122	45	140	510	1.500E+07	1.284E+06	2600	650	6.916	RT3	1780.81	31.51 %	rock avalanche	Xu et al. 2009a; Fan and Qiao 2010; Qi et al. 2011
8	N32.431, E105.109	35	166	260	8.575E+06	4.970E+05	1829	710	6.316	RT3	999.72	45.34 %	Rock avalanche	Xu et al. 2009a; Li et al. 2010; Li and Kong 2010
9	N32.451, E105.193	45	168	180	1.575E+06	4.145E+05	350	212	7.232	RT4	535.67	53.05 %	Soil slide	
10	N31.816, E104.448	52	140	602	1.400E+06	1.254E+05	1166	788	10.367	RT4	893.06	23.41 %	Rock avalanche	Xu et al. 2009a; Li et al. 2010; Li and Kong 2010
11	N31.647, E104.278	40	147	348	2.402E+06	1.101E+05	593	372	6.601	RT1	2208.21	272.38 %	Rock slide	Xu et al. 2009a; Li et al. 2010; Li and Kong 2010
12	N31.622, E104.141	50	165	310	1.500E+07	3.532E+05	1000	831	9.404	RT3	1115.42	11.54 %	Rock avalanche	Xu et al. 2009a
13	N31.830, E104.459	35	165	350	2.400E+06	1.300E+05	680	350	9.536	RT3	833.43	22.56 %	Rock slide	Yin et al. 2009; Xu et al. 2009a
14	N31.919, E104.576	40	165	200	1.600E+06	4.711E+05	545	305	9.572	RT4	571.38	4.84 %	Debris avalanche	Xu et al. 2009a
15	N32.309, E104.966	21	168	250	1.200E+07	6.957E+05	2043	570	6.600	RT2	1383.66	32.27 %	Rock avalanche	Xu et al. 2009a
16	N31.045, E103.458	41	149	420	7.500E+06	5.277E+05	3300	950	10.820	RT1	2552.87	22.64 %	Rock avalanche	Xu et al. 2009a; Qi et al. 2011
17	N31.553, E104.135	40	153	380	2.750E+07	2.946E+06	4170	1360	6.638	RT3	1558.04	62.64 %	Rock avalanche	Xu et al. 2009a
18	N31.397, E103.841	45	143	550	2.500E+06	2.943E+05	1730	850	9.469	RT2	1742.32	0.71 %	Debris avalanche	Xu et al. 2009a
19	N31.508, E104.226	43	168	254	3.449E+06	2.299E+05	1500	500	3.888	RT3	829.78	44.68 %	Rock slide	
20	N32.177, E104.821	35	155	450	3.520E+06	2.380E+05	550	345	7.156	RT4	790.78	43.78 %	Soil slide	Fan and Qiao 2010

Table 3 (continued)

No.	Latitude, longitude	Slope angle, θ ($^{\circ}$)	Slope transition angle, β ($^{\circ}$)	Slope height, h (m)	The volume of sliding source, V (m^3)	The area of sliding source, A (m^2)	Travel distance, L_{max} (m)	Landslide height, H_{max} (m)	PHA (m/s^2)	Rock type, RT	Predicted L_{max} (m)	Error (%)	Landslide type	Reference
21	N32.093, E104.724	30	165	180	6.670E+05	5.973E+04	510	280	7.480	RT4	497.15	2.52 %	Soil slide	
22	N32.091, E104.780	35	163	200	7.500E+05	7.106E+04	567	350	8.835	RT4	527.65	6.94 %	Soil slide	
23	N32.704, E105.538	22	174	220	7.240E+05	1.206E+05	641	380	7.286	RT2	780.54	21.77 %	Rock slide	
24	N31.628, E104.342	25	171	200	6.370E+05	2.548E+05	1440	500	4.567	RT2	814.73	43.42 %	Debris avalanche	
25	N31.605, E104.198	46	150	200	2.418E+05	8.061E+04	803	210	7.903	RT2	1061.52	32.19 %	Rock avalanche	
26	N31.911, E104.550	55	170	300	1.445E+07	4.817E+05	824	380	9.103	RT3	999.52	21.30 %	Soil slide	
27	N31.444, E104.018	29	173	250	1.956E+06	1.304E+05	825	400	6.327	RT2	933.71	13.18 %	Rock slide	
28	N32.426, E105.036	42	176	145	2.541E+05	1.271E+05	830	300	5.500	RT3	463.17	44.20 %	Debris avalanche	
29	N32.345, E105.037	37	164	120	1.219E+05	6.094E+04	873	260	6.970	RT3	529.58	39.34 %	Debris avalanche	
30	N32.298, E105.044	40	148	200	4.778E+05	1.195E+05	836	300	8.411	RT4	656.01	21.53 %	Debris avalanche	
31	N31.855, E104.306	39	157	300	3.484E+06	2.903E+05	839	520	5.915	RT3	1038.52	23.78 %	Soil slide	
32	N31.516, E103.551	40	152	400	6.016E+05	2.005E+05	1107	600	3.580	RT3	864.51	21.90 %	Debris avalanche	
33	N32.264, E104.925	28	165	290	6.352E+06	4.234E+05	1128	550	6.910	RT2	1330.55	17.96 %	Rock avalanche	
34	N32.634, E105.518	42	151	380	6.002E+05	2.401E+05	1131	500	8.870	RT3	880.50	22.15 %	Debris avalanche	
35	N31.833, E104.230	35	175	237	1.202E+07	6.011E+05	1222	430	5.401	RT2	1194.71	2.23 %	Debris avalanche	
36	N31.845, E104.492	40	157	320	4.354E+06	5.984E+05	1433	860	10.053	RT3	1075.98	24.91 %	Rock avalanche	Li and Kong 2010; Qi et al. 2011
37	N31.302, E103.838	38	162	240	1.007E+06	3.357E+05	1635	730	6.047	RT1	1443.24	11.73 %	Rock avalanche	Qi et al. 2011
38	N31.510, E104.137	47	174	400	4.738E+05	1.579E+05	1156	740	5.511	RT2	729.64	36.88 %	Rock avalanche	Qi et al. 2011
39	N31.660, E104.237	27	173	257	3.000E+06	1.694E+05	1180	485	10.465	RT2	999.43	15.30 %	Rock avalanche	Xu et al. 2009a; Fan and Qiao 2010
40	N31.527, E103.770	34	170	421	9.100E+06	1.820E+06	580	391	4.940	RT4	679.06	17.08 %	Soil slide	Li et al. 2010; Li and Kong 2010
41	N31.676, E104.360	40	172	180	4.500E+04	1.344E+05	501	200	5.540	RT2	523.42	4.47 %	Soil slide	
42	N31.919, E104.576	42	150	360	3.400E+06	2.429E+05	920	370	9.567	RT4	864.18	6.07 %	Debris avalanche	Xu et al. 2009a
43	N31.919, E104.576	41	149	300	3.000E+06	2.727E+05	700	340	9.577	RT4	862.82	23.26 %	Debris avalanche	Xu et al. 2009a
44	N32.278, E104.941	37	166	140	6.500E+05	3.700E+04	400	180	6.867	RT3	663.30	65.82 %	Rock avalanche	Xu et al. 2009a; Yuan et al. 2011
45	N31.516, E104.222	46	167	391	9.750E+05	6.500E+04	542	468	4.080	RT3	693.00	27.86 %	Rock slide	Li et al. 2009, 2010; Li and Kong 2010
46	N32.222, E104.467	45	155	280	3.519E+05	8.796E+04	486	380	3.448	RT4	548.27	12.81 %	Soil slide	Qi et al. 2011

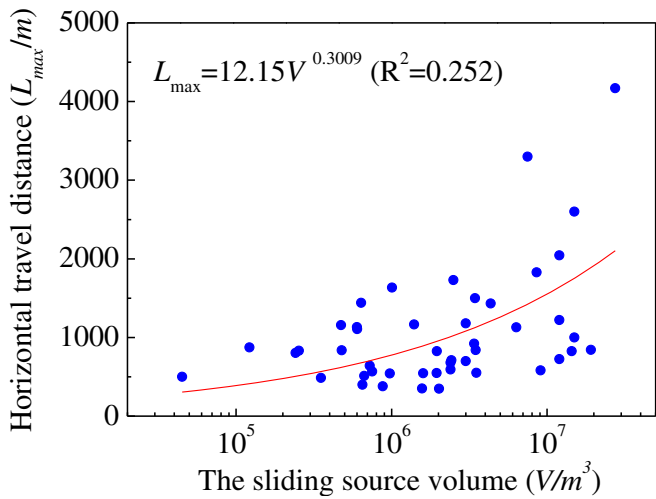


Fig. 4 Landslide travel distance related with sliding source volume

$$\log L_{\max} = 0.136RT + 0.159\log V + 0.529\sin\beta + 1.497 \quad (R^2 = 0.51) \quad (2)$$

However, coefficient of determination (R^2) indicates the regressive correlation of optimization empirical model is moderate; its validity need to be confirmed. By using Eq. (2) to predict the travel distance of surveyed 46 landslides, the comparison between predictions and observations was shown in Fig. 8; the estimation error of each landslide, $|L_{\text{predicted}} - L_{\text{observed}}| / L_{\text{observed}} \times 100\%$, was listed in the column of "Error" in Table 3. This self-verification suggests that proposed statistical model for travel distance prediction is valid for most landslides. In order to further verify its applicability, eight landslides in Wenchuan earthquake area were used to check the validity of Eq. (2); the parameters of each landslides and the predictive results were listed in Table 5, and the corresponding eight landslides were compared; their observed and predicted travel distances in Fig. 8, which further suggest that the proposed model may be valid. Therefore, it might be useful to preliminarily assess the travel distance of potential

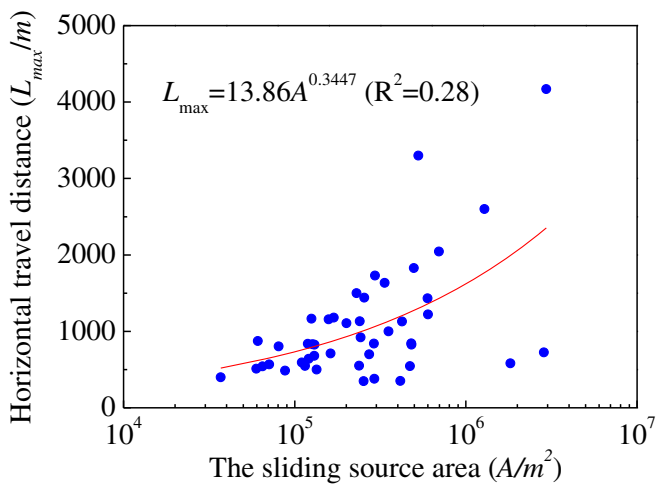


Fig. 5 Landslide travel distance related with sliding source area

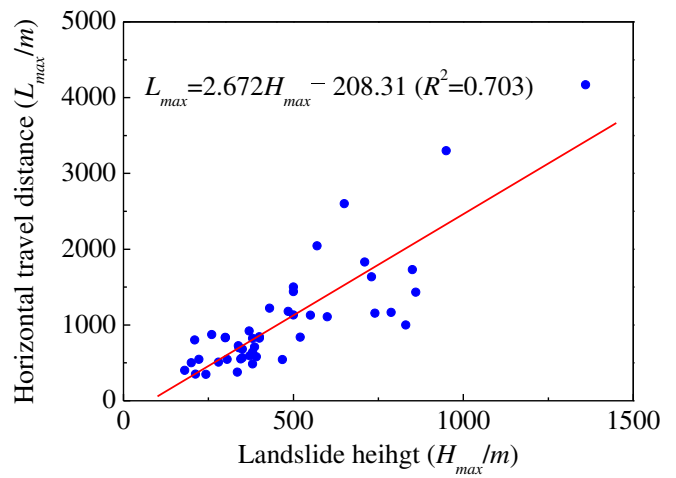


Fig. 6 Landslide travel distance related with landslide height

landslide in Wenchuan earthquake area and other similar geological and geomorphological regions. Nevertheless, the reliability of this empirical model needs to be further verified by some techniques, such as ROC curves and success rate curves (Frattoni et al. 2010).

Discussions

Based on the empirical model, it suggests that landslide travel distance had positive correlation with rock type (from soft rock to hard rock), landslide volume, and the sine of slope transition angle. It was inferred that landslide consisting of much softer rock (RT smaller), more kinetic energy would be consumed by friction, then failed mass would have shorter travel distance. The relation between landslide volume and travel distance was shown in Fig. 9 besides the data from Wenchuan earthquake, which reveals that landslide travel distance increased with landslide volume. Regarding the correlation between travel distance and the sine of slope transition angle, when a slope had several sections with different inclination, the failed mass would impact at the portion

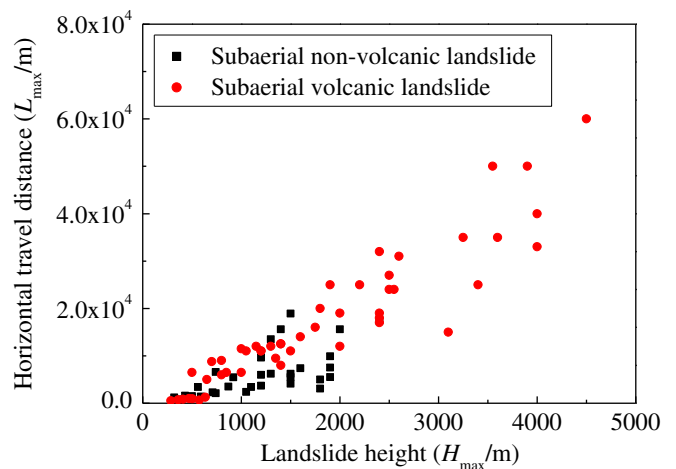


Fig. 7 The relations between travel distance and total elevation loss of nonvolcanic and volcanic landslides (data from Hayashi and Self 1992; Legros 2002)

Table 4 Multiple analysis of landslide travel distance by backward elimination approach

$\log L_{\max} = n_1 R T + n_2 \log V + n_3 \sin \beta + n_4 \log h + n_5 \log PHA + n_6 \tan \theta + n_0$												
Variable and parameter	n_1	n_2	n_3	n_4	n_5	n_6	n_0	Multiple R	F-stat	$F_{0.05}$	t test ($t_{0.05}$)	
six variables	n_i	0.139	0.189	0.618	-0.182	-0.133	0.049	1.795				
	t-stat	4.439	3.280	2.749	-0.737	-0.555	0.351	3.544	0.719	6.973	2.342	2.023
	\hat{n}_i	0.507	0.475	0.403	-0.120	-0.070	0.044	-				
five variables	n_i	0.137	0.185	0.633	-0.165	-0.125	-	1.811				
	t-stat	4.491	3.312	2.911	-0.689	-0.530	-	3.630	0.718	8.530	2.449	2.021
	\hat{n}_i	0.501	0.465	0.413	-0.109	-0.066	-	-				
four variables	n_i	0.137	0.176	0.584	-0.129	-	-	1.686				
	t-stat	4.534	3.324	2.994	-0.568	-	-	3.867	0.716	10.781	2.600	2.020
	\hat{n}_i	0.501	0.444	0.381	-0.085	-	-	-				
three variables	n_i	0.136	0.159	0.529	-	-	-	1.497				
	t-stat	4.539	3.692	3.150	-	-	-	5.345	0.713	14.501	2.827	2.018
	\hat{n}_i	0.496	0.401	0.345	-	-	-	-				

of slope transition. The fragment effect due to impact would enable failed mass to become high mobility, then making landslide travel longer. The range of slope transition angle of surveyed landslides was within $140^\circ \sim 176^\circ$, with the decrease of slope transition angle (namely, the increment of $\sin \beta$); the fragment effect became more significant, causing failed mass to have higher mobility and travel longer. Therefore, landslide travel distance had positive relation with the sine of slope transition angle.

In order to directly estimate landslide travel distance, Rickenmann (1999) and Legros (2002) developed empirical models for this issue, being listed in Table 6. Making use of these two previous models to estimate landslide travel distance of these 54 landslides in Wenchuan earthquake area, the results were shown in Fig. 10. It suggests that the model proposed by Rickenmann

(1999) and Legros (2002) cannot obtain satisfactory assessment; the average errors of these two models are 248.26 and 116.77 %, respectively. From the above plot of Fig. 10, most of predicted travel distances by the model of Rickenmann (1999) are significantly longer than the observations (above the dash line with 2:1 gradient); this comparison suggests that the model proposed by Rickenmann is not suitable for the prediction of landslides triggered by the 2008 Wenchuan earthquake because Rickenmann model is based on debris flow dataset. However, dataset in this paper mainly included rock (soil) slide and debris (rock) avalanche; therefore, it may draw a conclusion that the mechanism of debris flow is very different from rock (soil) slide and debris (rock) avalanche and results in the failed application of Rickenmann model in Wenchuan earthquake area; on the other hand, most of predictions by Rickenmann model are significantly bigger than the observations (above the dash line with 2:1 gradient), and there is no prediction smaller than observation; it means that under the same conditions (volume, rock type, and slope transition angle, etc.), debris flow usually will travel longer than rock (soil) slide and debris (rock) avalanche. The reason was inferred that the lubrication of water content in the failed mass of debris flow increased travel distance. This comparison reconfirmed and implied that landslide travel distance was heavily affected by mobile mechanism of sliding mass, especially failed mass with relatively abundant water content; it would cause the mobilization of debris flow that was quite different from other types of landslides. For the model of Legros, its invalidity of usage in Wenchuan earthquake area might be due to the difference of geological and hydrogeological conditions.

The mobile motion of slope failure was affected by numerous factors, such as topography, rock (soil) properties, mobile mechanisms, ground water, and so on. As many influential factors as the authors could collect, 46 well-documented landslides with nine parameters were used to develop empirical model of landslide travel distance, and eight landslides were applied to

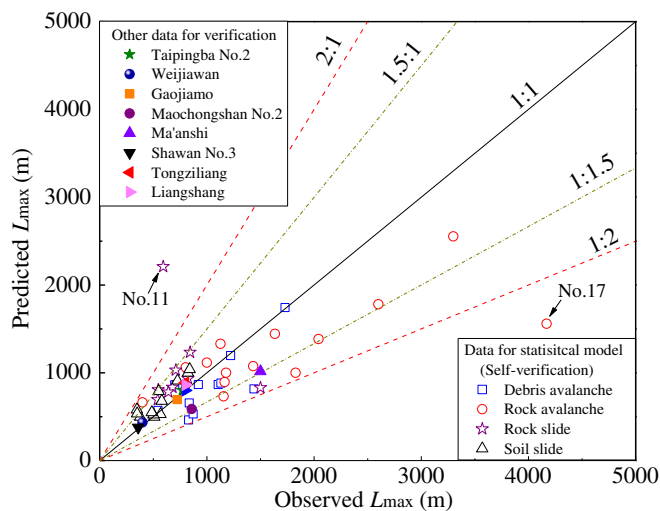


Fig. 8 Observed versus predicted horizontal travel distance

Table 5 The verification of proposed statistical model for landslide travel distance by case studies

Landslide	Slope transition angle, β (°)	Sliding volume, V (10^4 m ³)	Main lithology	Rock type, RT	H_{max} (m)	Observed L_{max} (m)	Predicted L_{max} (m)	Estimation error (%)	Reference
Taipingba no. 2	150	30	Weakly weathered phyllite	RT3 (RT=2)	540	770	802.35	4.20 %	Gou 2012
Weijiawan	172	10	Weakly weathered phyllite and limestone	RT3 (RT=2)	200	400	434.13	8.53 %	Gou 2012
Gaojiamo	168	113	Weakly weathered phyllite and limestone	RT3 (RT=2)	340	722	694.10	3.86 %	Gou 2012
Maochongshan no. 2	171	58	Weakly weathered metasandstone	RT3 (RT=2)	534	860	586.33	31.82 %	Gou 2012
Ma'anshi	151	148	Weakly weathered phyllite	RT3 (RT=2)	464	1500	1015.16	32.32 %	Gou 2012
Shawan no. 3	172	30	Moderately ~ strongly weathered metasandstone	RT4 (RT=1)	240	360	377.99	5.00 %	Gou 2012
Tongziliang	146	256	Moderately ~ strongly weathered metasandstone	RT4 (RT=1)	110	800	886.59	10.82 %	Gou 2012
Liangshang	155	600	Weakly weathered shale and moderately weathered limestone	RT4 (RT=1)	620	800	859.59	7.45 %	Gou 2012

verify the validity of presented model. Our data exclude landslides obstructed by relatively large river, valley, and infrastructures that neither included travel path sharply confined by steep side slope nor big deflection of travel path. However, it was difficult to judge the confinement degree during the investigation; the boundary between partly confined and confined not only relied on the experience of investigator but also affected by the relative magnitude between landslide volume and obstacles or

topographical changes; hence, the estimation error of several predictions was too large to be valid, such as landslide no. 11 and no. 17 in Table 3. Moreover, travel distance of 46 landslides in Table 3 is 91.3 % (42 out of 46) shorter than 2000 m; it may cause the predicted results of landslides with over 2,000 m observed travel distance that are more scattering than others in Fig. 8. However, compared with observations, the overall outcome by presented empirical model mainly yielded satisfactory results, which implies that the judgment about the degree of confinement during data collection and linear hypothesis for statistical model were both reasonable. One more reason for the scattering of comparison plot might be attributed to the discretization of data because some data are from field investigation and some data are from the published papers and books.

The limitation of this study is that the effects of ground water, geological structure, and landslide type on travel distance were not discussed. Previous studies have been found that pore-water pressure caused shear strength significant reduction (Takarada et al. 1999; Major and Iverson 1999; Wang and Sassa 2003; Sassa et al. 2004, 2005), and then resulting in failed mass might perform different mobile motions during sliding. The effect of geological structure on slope failure mode was demonstrated by Aydan and Hamada (2006, 2009), and Corominas (1996) proposed that different landslide types appeared different mobile abilities based on empirical relations of different landslide types. Therefore, discussion on landslide travel distance should consider the influence of geological structure and landslide type. However, in this paper, our data are limited to 54 landslides, and the types of slope failure mainly included rock (or soil) slide, rock avalanche,

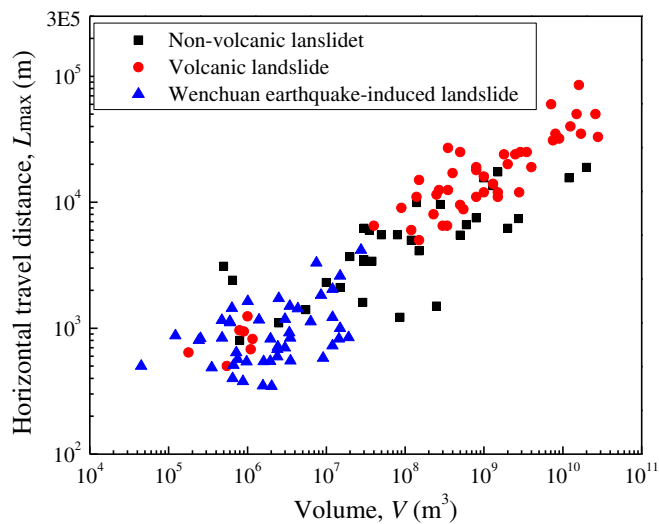


Fig. 9 The relation between landslide horizontal travel distance and volume [the data of nonvolcanic and volcanic landslide are from Hayashi and Self (1992) and Legros (2002)]

Table 6 Landslide travel distance prediction models and their comparisons

Prediction model	Data source	Authors	Average error for 54 surveyed landslides
$\log L_{\max} = 0.136RT + 0.159 \log V + 0.529 \sin \beta + 1.497$	46 landslides	This paper	29.99 %
$L_{\max} = 8V^{0.25}$	32 landslides	Legros 2002	116.77 %
$L_{\max} = 1.9V^{0.16}H_{\max}^{0.83}$	160 debris flows	Rickenmann 1999	248.26 %

V and L_{\max} in units of cubic meter and meter, respectively, except the model of Legros (2002), which V and L_{\max} is in cubic kilometer and kilometer

and debris avalanche. If these data were further classified into several groups, the regression model of each type of landslide would be uncertainty. Hence, a more generalized model of landslide was derived to estimated landslide travel distance. In spite of ignoring the influences of ground water, geological structure, and landslide type on landslide travel distance in proposed model, most of the predicted results are reasonable compared with observations, as listed in Table 3 and Fig. 8. Notwithstanding, the applicability of proposed model needs to be further verified, and more influential

factors on landslide travel distance were recommended to take into consideration during improvement.

Conclusions

In this study, the authors collected 54 well-documented landslides triggered by the 2008 Wenchuan earthquake, and landslides were delineated by following parameters, such as slope angle (θ), slope transition angle (β), slope height (h), horizontal travel distance (L_{\max}), landslide height (H_{\max}), the volume of sliding source (V) and sliding source area (A), rock type (RT), and horizontal peak ground acceleration (PHA). The results of multivariable analysis revealed that rock type, sliding source volume, and slope transition angle had predominant effect on landslide travel distance during Wenchuan earthquake and followed by slope height, seismic acceleration, and slope angle. An empirical model, as Eq. (2), was developed to predict landslide travel distance in similar geomorphological and geological region as Wenchuan earthquake affected area.

Acknowledgments

China Scholarship Council is deeply appreciated for supporting the first author to pursue his Ph.D. in Waseda University. The authors acknowledge the financial support provided by the Joint Fund of National Natural Science Foundation of China and High-speed Railway (no.U1134208), National Science and Technology Support Program (no.2012BAG05B03) and the National Basic Research (973) Program of China (no. 2010CB732105). The authors thank the reviewers and Dr. Liao for giving good comments to this paper. Anonymous researchers who timely conducted field survey after the 2008 Wenchuan earthquake were sincerely appreciated, and also, deep gratitude to the researchers who published their investigation results.

References

- Aydan O, Hamada M (2006) Damage to civil engineering structures by Oct.8,2005 Kashmir earthquake and recommendations for recovery and reconstruction. *J Disaster Res* 1(3):1–9
- Aydan O, Ohta Y, Hamada M et al (2009) The characteristics of the 2008 Wenchuan earthquake disaster with a special emphasis on rock slope failure, quake lakes and damage to tunnels. *J Sch Mar Sci Technol* 7(2):1–23, Tokai University
- Berti M, Simoni A (2007) Prediction of debris flow inundation areas using empirical mobility relationships. *Geomorphology* 90:144–161
- Corominas J (1996) The angle of reach as a mobility index for small and larger landslides. *Can Geotech J* 33:260–271
- Chang, SB, Zhang, SM, et al., 2006. *Manual of Engineering Geology* (Fourth edition), China architecture and building, 17–18, Beijing. (In Chinese)
- Chigira M, Wu XY, Inokuchi T, Wang GH (2010) Landslides induced by the 2008 Wenchuan earthquake, Sichuan, China. *Geomorphology* 118:225–238
- Dai FC, Xu Q, Yao X, Xu L, Tu XB, Gong QM (2011) Spatial distribution of landslides triggered by the 2008 Ms8.0 Wenchuan earthquake, China. *J Asian Earth Sci* 40:833–895

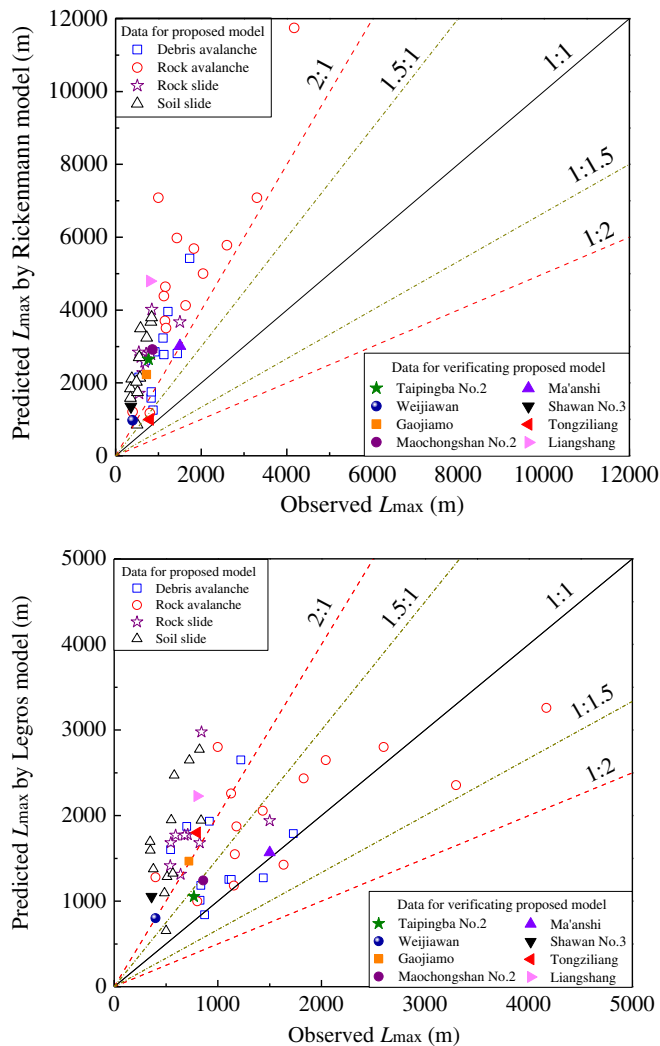


Fig. 10 Predicted landslide travel distance by two previous models versus the observed

- Finlay PJ, Mostyn GR, Fell R (1999) Landslide risk assessment: prediction of travel distance. *Can Geotech J* 36:556–562
- Fannin RJ, Wise MP (2001) An empirical–statistical model for debris flow travel distance. *Can Geotech J* 38:982–994
- Fan XY, Qiao JP (2010) Influence of landslide and ground factors on large-scale landslide movement. *Chin J Rock Mech Eng* 29(11):2337–2347 (In Chinese with English abstract)
- Frattini P, Crosta G, Carrara A (2010) Techniques for evaluating the performance of landslide susceptibility models. *Eng Geol* 111:62–72
- Gorum T, Fan XM, Westen CJ, Huang RQ, Xu Q (2011) Distribution pattern of earthquake-induced landslides triggered by the 12 May 2008 Wenchuan earthquake. *Geomorphology* 133:152–167
- Gou FG (2012) Regularity and risk analysis of landslides induced by Wenchuan earthquake—using a case of Pingtong-Naban segment, Chengdu University of Technology. (Master thesis, In Chinese with English abstract)
- Guo DP, Hamada M (2013) Qualitative and quantitative analysis on landslide influential factors during Wenchuan earthquake: a case study in Wenchuan County. *Eng Geol* 152:202–209
- Heim A (1932) *Bergsturz und Menschenleben*. Fretz und Wasmuth, Zurich, p 218
- Hayashi JN, Self S (1992) A comparison of pyroclastic flow and landslide mobility. *J Geophys Res* 97:9063–9071
- Hunter G, Fell R (2003) Travel distance angle for “rapid” landslides in constructed and natural soil slopes. *Can Geotech J* 40:1123–1141
- Huang RQ, Li WL (2008) Research on development and distribution rules of geohazards induced by Wenchuan earthquake on 12th May, 2008. *Chin J Rock Mech Eng* 27(12):2585–2592 (In Chinese with English abstract)
- Huang RQ, Li WL (2009a) Analysis on the number and density of landslides triggered by the 2008 Wenchuan earthquake, China. *J Geol Hazards Environ Preserv* 20(3):1–7 (In Chinese with English abstract)
- Huang RQ, Li WL (2009b) Analysis of the geo-hazards triggered by the 12 May 2008 Wenchuan earthquake, China. *Bull Eng Geol Environ* 68:363–371
- Hattanji T, Moriwaki H (2009) Morphometric analysis of relic landslides using detailed landslide distribution maps: implications for forecasting travel distance of future landslides. *Geomorphology* 103:447–454
- Hattanji T, Moriwaki H (2011) Topographic features and mobility of old landslides in Tanzania and Hakone areas—focusing on equivalent coefficient of dynamic friction and areal expansion of landslide mass. *J Jpn Landslide Soc* 48(1):45–51 (In Japanese with English abstract)
- Ji C., Hayes G (2008) Finite fault model-preliminary result of the May 12, 2008 Mw7.9 eastern Sichuan, China earthquake. Information from website: http://earthquake.usgs.gov/earthquakes/eqinthenews/2008/us2008ryan/finite_fault.php
- Kokusho T, Motoyama R, Motoyama H (2007) Wave energy in surface layers for energy-based damage evaluation. *Soil Dyn Earthq Eng* 27:354–366
- Kokusho T, Ishizawa T, Nishida K (2009) Travel distance of failed slopes during 2004 Chuetsu earthquake and its evaluation in terms of energy. *Soil Dyn Earthq Eng* 29:1159–1169
- Legros F (2002) The mobility of long-runout landslides. *Eng Geol* 63:301–331
- Li XZ, Kong JM, Deng HY et al (2009) Analysis on characteristics and deformation failure mode of large-scale landslides induced by “5·12” Wenchuan earthquake. *J Sichuan Univ (Eng Sci Ed)* 41(3):72–77 (In Chinese with English abstract)
- Li XZ, Kong JM (2010) Runout distance estimation of landslides triggered by “5·12” Wenchuan earthquake. *J Sichuan Univ (Eng Sci Ed)* 42(5):243–249 (In Chinese with English abstract)
- Li XZ, Kong JM, Cui Y, Tian SJ (2010) Statistical relations between landslides induced by Wenchuan earthquake and earthquake parameters, geological as well as geomorphological factors. *J Eng Geol* 18(1):8–14 (In Chinese with English abstract)
- Major JJ, Iverson RM (1999) Debris-flow deposition: effects of pore-fluid pressure and friction concentrated at flow margins. *Geol Soc Am Bull* 111:1424–1434
- McDougall SD, Hungr O (2003) Objectives for the development of an integrated three-dimensional continuum model for the analysis of landslide runout. In: Rickenmann D, Chen C-L (eds) *Proceedings of the third international conference on debris flow hazard mitigation: mechanics, prediction, and assessment*. Davos Mill, Rotterdam, pp 481–490
- Okura Y, Kitahara H, Kawanami A, Kurokawa U (2003) Topography and volume effects on travel distance of surface failure. *Eng Geol* 67:243–254
- Prochaska AB, Santi PM, Higgins JD, Cannon SH (2008) Debris-flow runout predictions based on the average channel slope (ACS). *Eng Geol* 98:29–40
- Qi SW, Xu Q, Lan HX, Zhang B, Liu JY (2010) Spatial distribution analysis of landslides triggered by 2008.5.12 Wenchuan earthquake, China. *Eng Geol* 116:95–108
- Qi SW, Xu Q, Zhang B et al (2011) Source characteristics of long runout rock avalanches triggered by the 2008 Wenchuan earthquake, China. *J Asian Earth Sci* 40:896–906
- Rickenmann D (1999) Empirical relationships for debris flows. *Nat Hazards* 19:47–77
- Rickenmann D (2005) Runout prediction methods. In: Jakob M, Hungr O (eds) *Debris-flow hazards and related phenomena*. Praxis, Chichester, pp 305–324
- Roering JJ, Kirchner JW, Dietrich WE (2005) Characterizing structural and lithologic controls on deep-seated landsliding: implications for topographic relief and landscape evolution in the Oregon Coast Range, USA. *Geol Soc Am Bull* 117:654–668
- Shreve RL (1968) The Blackhawk landslide. *Geological Society of America. Spec pap* 108:1–47
- Scheidegger AE (1973) On the prediction of the reach and velocity of catastrophic landslides. *Rock Mech* 5:231–236
- Shaller PJ (1991) Analysis and implications of large martian and terrestrial landslides, Doctor thesis, California institute of Technology.
- Sassa K, Wang GH, Fukuoka H et al (2004) Landslide risk evaluation and hazard zoning for rapid and long-travel landslides in urban development areas. *Landslides* 1:221–235
- Sassa K, Fukuoka H, Wang F, Wang GH (2005) Dynamic properties of earthquake-induced large-scale rapid landslides within past landslide masses. *Landslides* 2:125–134
- Takahashi T (1981) Estimation of potential debris flows and their hazardous zones; soft countermeasures for a disaster. *Nat Disaster Sci* 3:57–89
- Takahashi T (1991) Debris flow. A.A. Balkema, Rotterdam
- Takarada S, Ui T, Yamamoto Y (1999) Depositional features and transportation mechanism of valley-filling Iwasegawa and Kaida debris avalanches. *Jpn Bull volcanology* 60:508–522
- Wang GH, Sassa K (2003) Pore-pressure generation and movement of rainfall-induced landslides: effects of grain size and fine-particle content. *Eng Geol* 69:109–125
- Wang KL, Lin ML (2011) Initiation and displacement of landslide induced by earthquake—a study of shaking table model slope test. *Eng Geol* 122:106–114
- Xu Q, Pei XJ, Huang RQ et al (2009a) Larger-scale landslides induced by the Wenchuan earthquake. Science, Beijing (In Chinese)
- Xu C, Dai FC, Yao X, Chen J, Tu XB, Sun Y, Wang ZY (2009b) GIS-based landslide susceptibility assessment using analytical hierarchy process in Wenchuan earthquake region. *Chinese Journal of Rock Mechanics and Engineering* 28(Supp. 2):1–8, In Chinese with English abstract
- Xu C, Dai FC, Yao X, Chen J, Tu XB, Cao YB, Xiao JZ (2010) GIS based certainty factor analysis of landslide triggering factors in Wenchuan earthquake. *Chinese Journal of Rock Mechanics and Engineering* 29(Supp. 1):2972–2981, In Chinese with English abstract
- Xu C, Xu XW, Yao X, Dai FC (2013) Three (nearly) complete inventories of landslides triggered by the May 12, 2008 Wenchuan Mw 7.9 earthquake of China and their spatial distribution statistical analysis. *Landslides*. doi:10.1007/s10346-013-0404-6
- Yin YP, Wang FW, Sun P (2009) Landslide hazards triggered by the 2008 Wenchuan earthquake, Sichuan, China. *Landslides* 6:139–151
- Yuan JK, Huang RQ, Pei XJ et al (2011) Characteristics and cause analysis of the Pingxi landslide triggered by the Wenchuan earthquake. *Hydrogeol Eng Geol* 38(3):110–115 (In Chinese with English abstract)

D. Guo (✉) · C. He · Y. Zou

Key Laboratory of Transportation Tunnel Engineering, Ministry of Education, Southwest Jiaotong University, Chengdu 610031, China
e-mail: guodeping99@gmail.com

D. Guo · M. Hamada

Department of Civil and Environmental Engineering, Waseda University, 3-4-10kubo, Shinjuku-ku, Tokyo 169-8555, Japan

Y. Wang

Department of Geological Engineering, Southwest Jiaotong University, Chengdu 610031, China